Author(s): Erickson, Jeremy D.; Vasko, Petra; Riparetti, Ryan D.; Fettinger, James C.; Tuononen, Heikki; Power, Philip P.

Title: Reactions of m-Terphenyl-Stabilized Germylene and Stannylene with Water and Methanol: Oxidative Addition versus Arene Elimination and Different Reaction Pathways for Alkyl- and Aryl-Substituted Species

Year: 2015

Version:

Please cite the original version:

Erickson, J. D., Vasko, P., Riparetti, R. D., Fettinger, J. C., Tuononen, H., & Power, P. P. (2015). Reactions of m-Terphenyl-Stabilized Germylene and Stannylene with Water and Methanol: Oxidative Addition versus Arene Elimination and Different Reaction Pathways for Alkyl- and Aryl-Substituted Species. Organometallics, 34(24), 5785-5791. https://doi.org/10.1021/acs.organomet.5b00884

Reactions of *m*-Terphenyl Stabilized Germylene and Stannylene with Water and Methanol: Oxidative Addition versus Arene Elimination and Different Reaction Pathways for Alkyl and Aryl Substituted Species

Jeremy D. Erickson,† Petra Vasko,‡ Ryan D. Riparetti,† James C. Fettinger,† Heikki M. Tuononen,‡,* and Philip P. Power†,*

† Department of Chemistry, University of California at Davis, One Shields Avenue, Davis, California 95616, United States

‡ Department of Chemistry, Nanoscience Center, University of Jyväskylä, P.O. Box 35, FI-40014 University of Jyväskylä, Finland

Supporting Information Placeholder

ABSTRACT: Reactions of the divalent germylene $Ge(Ar^{Me6})_2$ ($Ar^{Me6} = C_6H_3$-2,6-{C_6H_2-2,4,6-$(CH_3)_3$}$_2$) with water or methanol gave the Ge(IV) insertion products $(Ar^{Me6})_2Ge(H)OH$ (**1**) or $(Ar^{Me6})_2Ge(H)OMe$ (**2**), respectively. In contrast, its stannylene congener $Sn(Ar^{Me6})_2$ reacted with water or methanol to produce the Sn(II) species {$Ar^{Me6}Sn(\mu\text{-}OH)$}$_2$ (**3**) or {$Ar^{Me6}Sn(\mu\text{-}OMe)$}$_2$ (**4**), respectively, with elimination of $Ar^{Me6}H$. Compounds **1**–**4** were characterized by IR and NMR spectroscopy as well as by X-ray crystallography. Density functional theory calculations yielded mechanistic insight into the formation of $(Ar^{Me6})_2Ge(H)OH$ and {$Ar^{Me6}Sn(\mu\text{-}OH)$}$_2$. The insertion of an *m*-terphenyl stabilized germylene into the O–H bond was found to be catalytic, aided by a second molecule of water. The lowest energy pathway for the elimination of arene from the corresponding stannylene involved sigma-bond metathesis rather than separate oxidative addition and reductive elimination steps. The reactivity of $Sn(Ar^{Me6})_2$ with water or methanol contrasts with that of Sn{$(CH(SiMe_3)_2)_2$}$_2$ which affords the Sn(IV) insertion products {$(Me_3Si)_2CH$}$_2Sn(H)OH$ or {$(Me_3Si)_2CH$}$_2Sn(H)OMe$. The differences were tentatively ascribed to the Lewis basicity of the employed solvent (Et_2O vs. THF) and the use of molar vs. millimolar concentrations of the substrate.

INTRODUCTION

Stable divalent group 14 carbene analogues (tetrylenes) have attracted much interest over the last four decades.[1] Some of the more recent advances in this area include the synthesis of two-coordinate acyclic silylenes,[2] the donor–acceptor stabilization of heavy group 14 hydrides GeH_2 and SnH_2,[3] and the characterization of two-coordinate 1,2-bis-metalylenes,[4] a heavier analogue of 1,2-dicarbenes. The interest in stable tetrylenes is in part due to their facile and in some cases reversible reactivity with fundamentally important small molecules such as CO,[5] H_2,[2a,4,6] NH_3,[6a,7] and C_2H_4[8] under mild conditions. Of particular significance have been insertion reactions of which topical examples include the insertion of a silylene into a P–P bond of P_4,[9] the insertion of a cationic metallogermylene into X–H bonds (X = H, B, or Si),[10] and the insertion of a boryl substituted stannylene into the C≡C bond in alkynes.[11]

In recent years, we have carried out detailed investigations of the reactivity of *m*-terphenyl stabilized heavier tetrylenes with small molecules.[12] In this context, we have reported the reactions of $E(Ar^{Me6})_2$ (E = Ge, Sn; $Ar^{Me6} = C_6H_3$-2,6-{C_6H_2-2,4,6-$(CH_3)_3$}$_2$)[13] with H_2,[6] NH_3,[6a] CO,[5] isocyanides,[14] hydrazines,[15] inorganic acids HX (X = CN^-, N_3^-, F^-, $SO_3CF_3^-$, and BF_4^-),[16] and $AlMe_3$ and $GaMe_3$.[17] A logical extension of this chemistry is the investigation of the reactions of $E(Ar^{Me6})_2$ with hydroxyl compounds and of water and methanol in particular. Although the insertion of transient tetrylenes such as EH_2, EMe_2, or EPh_2 (E = Si, Ge, or Sn) into O–H bonds has been studied both experimentally and theoretically,[18] there are only a few examples of similar reactions involving stable acyclic tetrylenes that yield structurally characterized products. Most notably, Lappert *et al.* have reported the crystallographic characterization of {$(Me_3Si)_2CH$}$_2Ge(H)OEt$ from the reaction of Ge{$CH(SiMe_3)_2$}$_2$ with ethanol,[19] while Pörschke *et al.* obtained {$(Me_3Si)_2CH$}$_2Sn(H)OH$ by reacting Sn{$CH(SiMe_3)_2$}$_2$ with excess water.[20] A related species {$L(H)_2GeGe(H)(OH)L$}•(OEt_2) (L = C_6H_2-4-Me-2,6-{$C(H)Ph_2$}$_2$) was recently described by Jones et al. as a minor side product from the reaction of LGeGeL with H_2 in the presence of adventitious moisture.[4] In addition, insertion reactions of Ge{$CH(SiMe_3)_2$}$_2$ into the O-H bond of the enolic forms of several ketones have been reported, although none of the products has been structurally characterized.[21]

We now describe the reaction of $E(Ar^{Me6})_2$ (E = Ge, Sn) with water or methanol which give the insertion products $(Ar^{Me6})_2Ge(H)OR$ (**1**, R = H; **2**, R = Me) or the dimers {$Ar^{Me6}Sn(\mu\text{-}OR)$}$_2$ (**3**, R = H; **4**, R = Me) depending on the

group 14 element E (Scheme 1). The products **1**–**4** were characterized by spectroscopic methods and single crystal X-ray crystallography. The observed reactivity is similar to that seen for $E(Ar^{Me6})_2$ with NH_3[6a] and alkyl-amino tetrylenes [LEEt] (L = $N(C_6H_2$-4-Si^iPr_3-2,6-$\{C(H)Ph_2\}_2{}^iPr$)) with protic reagents,[22] but differs from that of $E(Ar^{Me6})_2$ with HBF_4, which resulted in the formation of an insertion product $(Ar^{Me6})_2E(H)F$ irrespective of the element E.[15] To shed light on the mechanistic details of the observed transformations, the reactions of stable germylenes and stannylenes with water were also probed computationally. The acquired experimental and computational results were compared with those reported for $E\{CH(SiMe_3)_2\}_2$ as well as with the data available for transient tetrylenes EMe_2 and EPh_2.

Scheme 1. Reaction of $E(Ar^{Me6})_2$ (E = Ge, Sn) with water or methanol to form **1**–**4**.

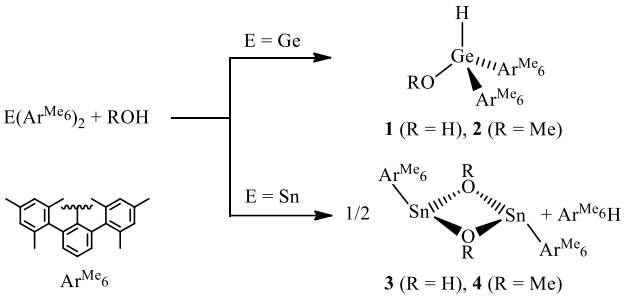

RESULTS AND DISCUSSION

The reaction of $Ge(Ar^{Me6})_2$ with water or methanol resulted in formal insertion of the germylene into the O–H bond to afford tetravalent $(Ar^{Me6})_2Ge(H)OH$ (**1**) or $(Ar^{Me6})_2Ge(H)OMe$ (**2**), respectively. In contrast, the reaction of $Sn(Ar^{Me6})_2$ with water or methanol gave the divalent dimers $\{Ar^{Me6}Sn(\mu\text{-}OH)\}_2$ (**3**) and$\{Ar^{Me6}Sn(\mu\text{-}OMe)\}_2$ (**4**), respectively, via elimination of $Ar^{Me6}H$.

Structures. Single crystal X-ray diffraction studies revealed a similar structural arrangement in **1** and **2** (Figures 1 and 2; selected structural data are given in Table 1). Compound **1** crystallizes in the orthorhombic *Fdd*2 space group, while the space group of the methoxy derivative **2** is monoclinic $P2_1/c$. In **1**, the germanium atom and the hydrogen and hydroxide groups bound to it are disordered over two sites with 50% occupancy. A similar distortion is seen in the structure of **2**, in which case the crystals were also found to contain co-crystallized **1** (18%) due to the presence of adventitious water in the reaction mixture.

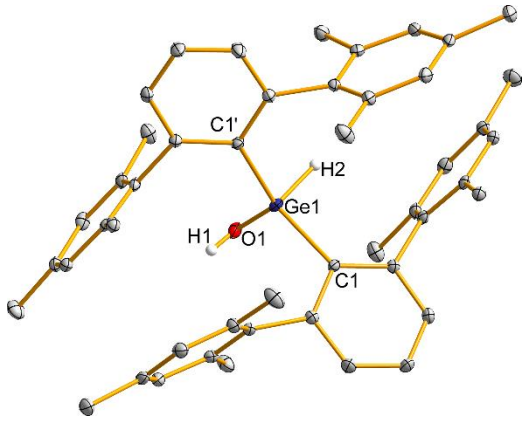

Figure 1. Thermal ellipsoid plot (30% probability) of **1**. Structural disorder and carbon-bound hydrogen atoms are not shown for clarity.

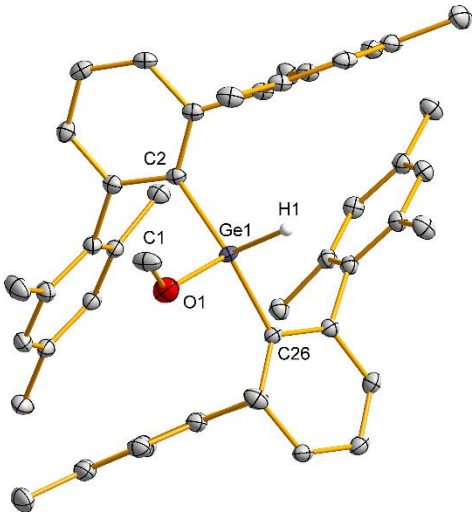

Figure 2. Thermal ellipsoid plot (30% probability) of **2**. Structural disorder and carbon-bound hydrogen atoms are not shown for clarity.

In both **1** and **2**, the germanium atom has tetrahedral coordination due to bonding to two terphenyl ligands, an oxygen atom from the hydroxyl/methoxy group, and a hydrogen atom. The germanium-bound hydrogen atom could not be clearly identified from the electron density difference map for either **1** or **2**, but its presence in the structures was confirmed with IR and ^1H NMR spectroscopies.

The structure of **1** can be compared to that of the related dihydroxy species $(Ar^{Me6})_2Ge(OH)_2$, synthesized by us,[23] and to $(Eind)_2Ge(H)OH$ (Eind = 1,1,3,3,5,5,7,7-octaethyl-s-hydridacen-4-yl) reported by Tamao, Matsuo, and coworkers through the reaction of the germanone $(Eind)_2GeO$ with $LiAlH_4$.[24] The Ge–O bond lengths in $(Ar^{Me6})_2Ge(OH)_2$ (1.782(3) and 1.803(3) Å) and in $(Eind)_2Ge(H)OH$ (1.757(2) Å) are equal to that in **1** (within 3σ), but the interligand C-Ge-C angles between organic substituents (123.04(6) and 122.5(3)º) are slightly more acute. The interligand C-Ge-C angle in **1** is also wider than that in the germylene precursor $Ge(Ar^{Me6})_2$ (114.2(2)°).[12] A comparison of the structure of **2** to that of $\{(Me_3Si)_2CH\}_2Ge(H)OEt$ shows their Ge–O bond lengths to be equal (1.797(5) Å in $\{(Me_3Si)_2CH\}_2Ge(H)OEt$).[18] However, the C-Ge-C interligand angles are significantly different (114.5(3)º in $\{(Me_3Si)_2CH\}_2Ge(H)OEt$, versus 136.33(7)° in **2**), most likely due to difference in the steric bulk of the Ar^{Me6} and $(Me_3Si)_2CH$ groups.

Compounds **3** and **4** crystallize in monoclinic space groups $C2/m$ and $P2_1/n$, respectively. Their structures revealed a dimeric arrangement with two $SnAr^{Me6}$ moieties bridged by two hydroxide (**3**) or methoxide (**4**) groups (Figures 3 and 4; selected structural data are given in Table 1). In contrast to compounds **1** and **2**, no structural disorder was observed either for **3** or **4**. However, crystals of the arene $Ar^{Me6}H$,[25] a side product in the synthesis of both **3** and **4**, were obtained together with **3** and **4** in all crystallizations.

The structures of **3** and **4** are similar with comparable structural parameters. Notable differences are only observed in the

orientation of the Ar^{Me6} ligands in relation to the four-membered Sn_2O_2 ring that is influenced by the steric requirements of the

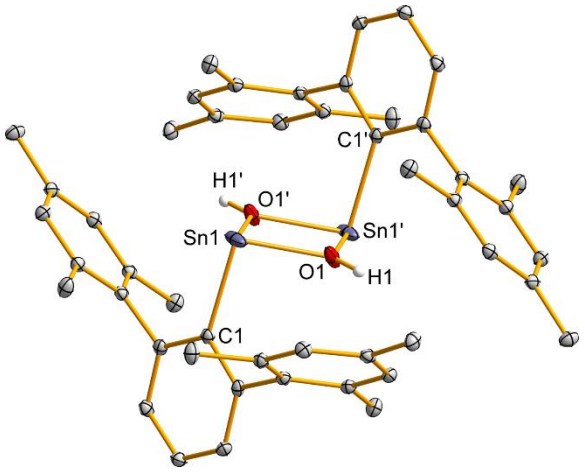

Figure 3. Thermal ellipsoid plot (30% probability) of **3**. Carbon-bound hydrogen atoms are not shown for clarity.

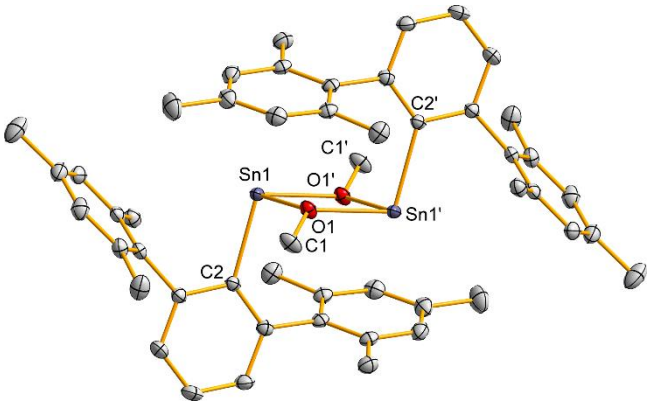

Figure 4. Thermal ellipsoid plot (30% probability) of **4**. Hydrogen atoms are not shown for clarity

Table 1. Selected bond lengths (Å) and angles (°) in products **1**–**4**.

1		**2**		**3**		**4**	
Ge1-O1	1.77(1)	Ge1-O1	1.797(2)	Sn1-O1	2.1345(14)	Sn1-O1	2.168(1)
		C1-O1	1.358(6)			C1-O1	1.430(2)
C1-Ge1-O1	109.1(5)	C26-Ge1-O1	98.81(8)	Sn1-C1	2.208(3)	Sn1-C2	2.256(2)
C1'-Ge1-O1	101.7(5)	C2-Ge1-O1	101.88(8)	C1-Sn1-O1	92.69(7)	C2-Sn1-O1	92.53(5)
		Ge1-O1-C1	123.9(3)	Sn1-O1-Sn1′	108.42(11)	Sn1-O1-Sn1′	107.67(5)
C1-Ge1-C1′	129.5(5)	C26-Ge1-C2	136.33(7)	O1-Sn1-O1′	71.58(11)	O1-Sn1-O1′	72.33(4)
				Sn1···Sn1'	3.4627(5)	Sn1···Sn1'	3.4801(7)

bridging hydroxide/methoxide group. In both **3** and **4**, the coordination around tin atoms is trigonal pyramidal with near 90° interligand C-Sn-O angles. We note that the structure of **3** is very similar to that of the related dimer $\{Ar^{iPr4}Sn(\mu\text{-}OH)\}_2$ (Ar^{iPr4} = C_6H_3-2,6-{C_6H_2-2,4-[$CH(CH_3)_2]_2$}$_2$) that was synthesized previously by us via reaction of a distannyne with TEMPO or pyridine-*N*-oxide.[26]

Spectroscopy. The ^{1}H NMR spectra of **1**–**4** display the characteristic signals of the Ar^{Me6} group with methyl and aromatic proton resonances appearing from 1.8 to 2.3 ppm and from 6.6 to 7.1 ppm, respectively (see Supporting Information).

The methoxy proton in **2** appears as a singlet at 2.74 ppm in the ^{1}H NMR spectrum, whereas the germanium-bound proton in **1** and **2** shows a resonance at 6.06 and 6.05 ppm, respectively. The Ge-OH proton chemical shift (0.47 ppm) was confirmed by COSY NMR spectroscopy. It is further upfield than that reported for the O–H proton $(Eind)_2Ge(H)OH$ (5.21 ppm), possibly as a result of shielding by the flanking rings. The Ge–H proton resonance was found to be a doublet with a coupling constant to the O–H proton of 1.4 Hz, confirming, albeit indirectly, the existence of the hydroxyl proton in the structure. The presence of the O–H proton is also supported by IR spectroscopy and the synthesis of the deuterium analogue of **1**, $(Ar^{Me6})_2Ge(D)OD$ (**1′**), via reaction of $Ge(Ar^{Me6})_2$ with D_2O (see Supporting Information). IR spectroscopy of **1′** showed the appearance of an O–D stretch at 2660 cm^{-1}, while the O–H stretch of **1** could be identified at 3600 cm^{-1}.

Products **3** and **4** could not be readily separated from the $Ar^{Me6}H$ byproduct to provide completely clean NMR spectra. This is due to the low solubility of **3** and **4** and the relatively high solubility of $Ar^{Me6}H$ to common solvents. Because of this, the NMR spectra of **3** and **4** were deconvoluted through comparison of the data to a spectrum of pure $Ar^{Me6}H$ (see Supporting Information). The methoxy proton in **4** appears as a singlet at 2.74 ppm in the ^{1}H NMR spectrum, while the O–H proton of **3** shows a resonance at 0.00 ppm. The latter assignment could be confirmed via synthesis of $\{Ar^{Me6}Sn(\mu\text{-}OD)\}_2$ (**3′**), the deuterium analogue of **3** (see Supporting Information). Even though the O–H stretch of **3** could not be seen in the IR spectrum at the expected region (*ca.* 3500 cm^{-1}),[24] the O–D stretch of **3′** is clearly visible at 2620 cm^{-1}.

While **1** and **2** are both colorless, products **3** and **4** are pale yellow and absorb in the near UV and violet region with λ_{max} of 365 and 302 nm for **3** and **4** (See Supporting Information).

Discussion. The observation of the dimeric products **3** and **4** parallels the reactivity of $Sn(Ar^{Me6})_2$ with NH_3.[6a] However, it differs from the results obtained by Pörschke and coworkers who found that the tin species $Sn\{CH(SiMe_3)_2\}_2$ undergoes simple insertion into both water and methanol,[20] forming

$\{(Me_3Si)_2CH\}_2Sn(H)OH$ and $\{(Me_3Si)_2CH\}_2Sn(H)OMe$, respectively. The germanium congener $Ge\{C(H)(SiMe_3)_2\}_2$ is also known to form insertion products $\{(Me_3Si)_2CH\}_2Ge(H)R$ (R = H, Me) analogous to **1** and **2**.[19] Hence, in order to understand the reactivity observed for $E(Ar^{Me6})_2$ with water or methanol, mechanistic investigations of possible reaction pathways were conducted computationally using density functional theory (DFT). The calculations were performed for model compounds $E(Ar^{Me4})_2$ (Ar^{Me4} = C_6H_3-2,6-$\{C_6H_3$-2,6-$(CH_3)_2\}_2$) as the *p*-methyl substituent in Ar^{Me6} is not expected to influence the reaction mechanism and can therefore be omitted to lower the computational cost.

Computational Results. Insertion into O–H bonds is one of the most studied reactions of transient silylenes and germylenes.[18] It has been shown both experimentally and theoretically that the reaction proceeds by formation of a Lewis acid-base complex, R'_2E'–OHR (E′ = Si, Ge; R′ = H, Me, Ph), followed by a proton transfer from oxygen to the group 14 element to give the O–H insertion product $R'_2E'(H)OR$. The latter step in the mechanism is not unimolecular but rather involves catalytic proton transfer by a second molecule of water or alcohol. An alternative reaction channel involving elimination of H_2 from water/alcohol complexes of parent tetrylenes, H_2E'–OHR, to yield HE'OR has also been identified computationally and experimentally verified by Leigh *et al.*[18a]

Calculations (PBE1PBE-D3BJ/def-TZVP) performed for the reaction of $E(Ar^{Me4})_2$ with water show that the formation of complexes $(Ar^{Me4})_2E$–OH_2 is slightly endergonic or energy neutral for E = Ge and Sn, respectively. The insertion into the O–H bond was found to take place catalytically, aided by a second molecule of water (Figure 5, left). This parallels the reactivity of transient tetrylenes with water/alcohols[18] or amines[28] as well as the mechanism calculated for the insertion of $Ge(Ar^{Me6})_2$ into the N–H bond in NH_3.[6a] The Gibbs energy of activation for the formation of $(Ar^{Me4})_2E(H)OH$ was found to be 46 and 73 kJ mol^{-1} for E = Ge and Sn, respectively. We note that the

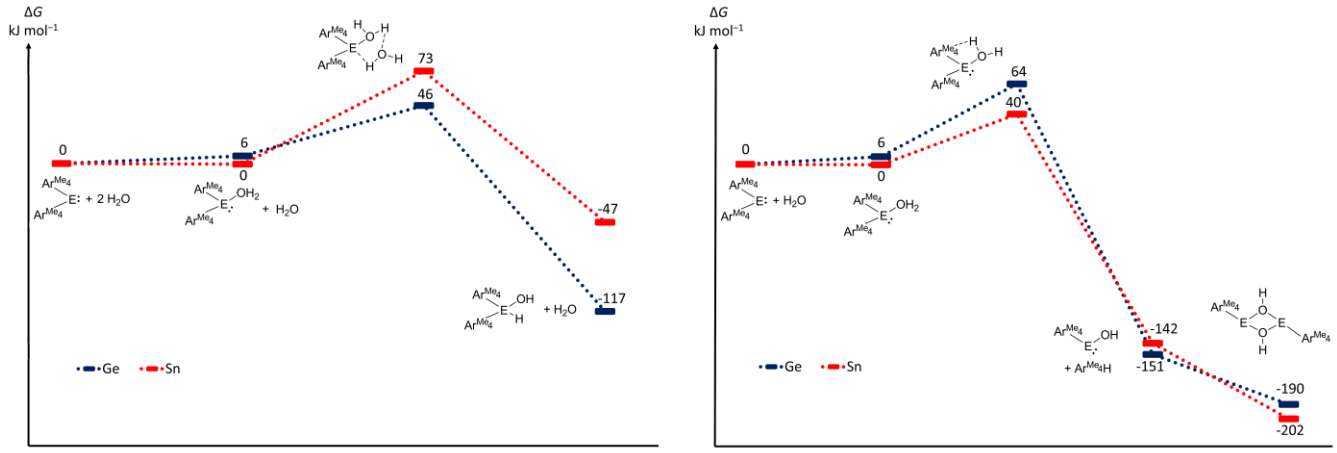

Figure 5. Energy diagrams (ΔG, kJ mol^{-1}) for the reactions of $(Ar^{Me4})_2E$ (E = Ge or Sn) with water leading to insertion into O–H bond and formation of $(Ar^{Me4})_2E(H)OH$ (left) or arene elimination and formation of $\{Ar^{Me4}E(\mu\text{-}OH)\}_2$ + $Ar^{Me4}H$ (right).

mechanism for a unimolecular proton transfer was found to have a considerably greater barrier, well above 100 kJ mol^{-1}, representing an improbable reaction pathway on the potential energy surface.

The arene elimination pathway (Figure 5, right) was calculated to proceed via one-step sigma bond metathesis[27] that has a Gibbs energy of activation of 64 and 40 kJ mol^{-1} for E = Ge and Sn, respectively. The reaction was found to proceed via a cyclic transition state in which a hydrogen from the coordinated water molecule in $(Ar^{Me4})_2E$–OH_2 is transferred to the aryl substituent, yielding $Ar^{Me4}EOH$ and $Ar^{Me4}H$. This is reminiscent of the mechanism calculated for the reaction of $Sn(Ar^{Me6})_2$ with NH_3 to give $Ar^{Me6}SnNH_2$.[6a] The hydroxytetrylene $Ar^{Me4}EOH$ can undergo a subsequent barrierless dimerization to form the hydroxide-bridged dimer $\{Ar^{Me4}E(\mu\text{-}OH)\}_2$ as the final product. We also tested the possibility that arene elimination would involve the product of the oxidative addition pathway. However, the energy barrier for elimination of $Ar^{Me4}H$ from $(Ar^{Me4})_2E(H)OH$ was found to be considerably higher than that calculated for the sigma bond metathesis.

A comparison of the two energy diagrams in Figure 5 shows that the oxidative insertion pathway has a lower barrier when E = Ge, whereas for E = Sn, the arene elimination pathway is kinetically favored. However, the dimer $\{Ar^{Me4}E(\mu\text{-}OH)\}_2$ is the thermodynamically preferred product independent of the identity of the group 14 element. As a whole, the computational results predict different reactivity for $Ge(Ar^{Me4})_2$ and $Sn(Ar^{Me4})_2$ with water, which is in good agreement with experimental observations. The lower energy barrier for $Ge(Ar^{Me4})_2$ in oxidative insertion can be rationalized with its greater Lewis basicity as compared to $Sn(Ar^{Me4})_2$. In a similar fashion, the barriers for reductive elimination parallel the strength of the E–C bond with the weaker bond corresponding to a lower barrier.

The computational results allow a straightforward rationalization as to why $Sn(Ar^{Me6})_2$ reacts with HBF_4 by simple insertion.[15] The elimination of $Ar^{Me6}H$ from $(Ar^{Me6})_2Sn(H)F$ would most likely proceed via high energy transition state, rendering such transformation unlikely. It is, however, less obvious why $Sn\{CH(SiMe_3)_2\}_2$ reacts with water or alcohol by oxidative insertion,[19] while $Sn(Ar^{Me6})_2$ undergoes arene elimination and subsequent dimerization to yield $\{Ar^{Me4}Sn(\mu\text{-}OR)\}_2$. For this reason, we also examined the reaction of $E\{CH(SiMe_3)_2\}_2$ with water using computational methods.

The results from DFT calculations (PBE1PBE-D3BJ/def-TZVP) suggested that the reaction of $E\{CH(SiMe_3)_2\}_2$ with water proceeds qualitatively similarly as observed for $E(Ar^{Me4})_2$ (see Supporting Information). Specifically, $Ge\{CH(SiMe_3)_2\}_2$ was predicted to react via oxidative insertion, whereas $Sn\{CH(SiMe_3)_2\}_2$ should eliminate $CH_2(SiMe_3)_2$ to give $\{(Me_3Si)_2HC\}SnOH$ that would readily dimerize to $[\{(Me_3Si)_2HC\}Sn(\mu\text{-}OR)]_2$. The dimer $[\{(Me_3Si)_2HC\}Sn(\mu\text{-}OR)]_2$ was found to be both the thermodynamically and kinetically favored product with a difference of 16 kJ mol^{-1} in activation energy for the two investigated pathways. We note that the energy barriers for the elimination of the alkane $CH_2(SiMe_3)_2$ were calculated to be approximately twice as high as those determined for the arene $Ar^{Me4}H$, as expected based on the differences in their electronic structures.

At this point we can only speculate as to why the experimental and computational results for the reactivity of $Sn\{CH(SiMe_3)_2\}_2$ with water differ. We note that the reactions of $Sn\{CH(SiMe_3)_2\}_2$ have used an excess (14 equivalents) of water at molar concentrations, [20] whereas strict 1:1 stoichiometry and only mM concentrations of substrate have been employed in all other instances, including this work. Thus, the reaction conditions of the present study favor elimination, while those of Pörschke *et al.* are set up to favor insertion.

It should also be pointed out that the experiments reported by Pörschke *et al.* employ THF as the solvent,[20] while the analogous reactions with $Ge\{CH(SiMe_3)_2\}_2$,[19] as well as those involving $E(Ar^{Me6})_2$, were performed in Et_2O and in the presence of millimolar quantities of the substrate. The properties of strong electron pair donor solvents are known to have significant influence to the reactivity of GeH_2 and $SiMe_2$, as the reacting species in such cases is not the free tetrylene but its Lewis acid–base adduct.[18a, 29] In a similar fashion, the product distribution from the reaction of $GePh_2$ with CCl_4 has been observed to depend on the employed solvent, with the insertion product $Ph_2Ge(Cl)CCl_3$ being favored in neat THF solutions or in hexanes containing catalytic amounts of THF;[30] with an even stronger donor, NEt_3, the insertion product was obtained exclusively. These data strongly suggest that the reactivity of $Sn\{CH(SiMe_3)_2\}_2$ with water or methanol could be vastly different if the reactions were carried out in Et_2O due to its less coordinating nature as compared to THF. Solvent modified reactivity of stable acyclic tetrylenes are currently under further computational and experimental investigations in our laboratories.

CONCLUSION

The *m*-terphenyl stabilized tetrylenes $Ge(Ar^{Me6})_2$ and $Sn(Ar^{Me6})_2$ were found to have differing reactivity towards both water and methanol. While the germylene $Ge(Ar^{Me6})_2$ inserts into the O–H bond to form the Ge(IV) products $(Ar^{Me6})_2Ge(H)OH$ (**1**) and $(Ar^{Me6})_2Ge(H)OMe$ (**2**), the corresponding stannylene $Sn(Ar^{Me6})_2$ undergoes arene elimination followed by dimerization to yield the Sn(II) species $\{Ar^{Me6}Sn(\mu\text{-}OH)\}_2$ (**3**) and $\{Ar^{Me6}Sn(\mu\text{-}OMe)\}_2$ (**4**). Computational analyses at the DFT level reproduced the experimental results and gave mechanistic insight into the formation of $(Ar^{Me6})_2Ge(H)OH$ and $\{Ar^{Me6}Sn(\mu\text{-}OH)\}_2$. The insertion of an Ar^{Me4} stabilized germylene into the O–H bond was found to be catalytic, aided by a second molecule of water. The lowest energy pathway for the elimination of arene from the corresponding stannylene involved sigma-bond metathesis rather than separate oxidative addition and reductive elimination steps. DFT calculations found no difference in the preferred reactivity of $Sn(Ar^{Me4})_2$ and $Sn\{CH(SiMe_3)_2\}_2$ even though the latter is known to undergo oxidative insertion into O–H bonds. A plausible explanation for the experimental behavior of the alkyl stannylene is the use of reaction conditions that favour insertion (molar concentrations of water and THF as the solvent).

EXPERIMENTAL SECTION

General Procedures. All manipulations were carried out in either an inert atmosphere glovebox or by using modified Schlenk techniques to maintain strictly anaerobic and anhydrous conditions. $Ge(Ar^{Me6})_2$ and $Sn(Ar^{Me6})_2$ were prepared by literature procedures.[13] Solvents were dried using a Grubbs-style purification system[31] and stored over NaK. Water was collected from a Thermo Scientific Barnstead Nanopure and degassed under reduced pressure (< 1 torr) for 2 h. Methanol was dried with CaH_2 and distilled onto 3 Å molecular sieves. ^1H and $^{13}C\{^1H\}$ spectra were recorded on a Bruker 500 MHz spectrometer and referenced to solvent signals. No ^{119}Sn signals could be observed in the region between +2400 and –1000 ppm. Melting points were determined on a Mel-Temp II apparatus using capillary tubes sealed with vacuum grease under an inert atmosphere. IR spectra were recorded as Nujol mulls between CsI plates on a Perkin-Elmer 1430 ratio recording infrared spectrometer. UV-Visible spectra were recorded from dilute solutions in toluene using 3 mL quartz cuvette and an Olis 17 modernized Cary 14 UV/Vis/NIR spectrophotometer.

$(Ar^{Me6})_2Ge(H)OH$ (1). H_2O (11.2 μL, 0.621 mmol) was dissolved in Et_2O (20 mL) and this solution was added dropwise to a slurry of $Ge(Ar^{Me6})_2$ (0.4343 g 0.621 mmol) in Et_2O (35 mL) at *ca.* −78 °C. The resulting mixture was stirred and allowed to warm to room temperature overnight, which resulted in a colorless solution. The solution was concentrated to *ca.* 5 mL and stored at *ca.* −28 °C to produce a colorless crystalline solid, **1**. Yield: 84% (0.373 g). Mp: 147−150 °C. ^1H NMR (500 MHz, C_6D_6, 25 °C, ppm): 0.47 (br s, 1H, O–*H*) 1.89 (s, 6H, *o*-Me), 1.94 (s, 6H, *o*-Me), 2.22 (s, 6H, *p*-Me), 6.06 (d, J_{HH} = 1.4 Hz, 1H, Ge-*H*), 6.65, (d, J_{HH} = 7.5 Hz, 4H, C_6H_3), 6.80 (s, 4H, C_6H_2), 6.81 (s, 4H, C_6H_2), 6.99 (t, J_{HH} = 7.5 Hz, 2H, C_6H_3). $^{13}C\{^1H\}$ NMR (151 MHz, C_6D_6, 25 °C, ppm): 21.27 (*p*-CH_3), 22.05 (*o*-CH_3), 22.16 (*o*-CH_3), 128.35, 128.75, 129.65, 130.25, 136.72, 136.99, 137.05, 138.74, 140.69, 148.27. IR (cm^{-1}): 3600 (w), 3000 (s), 2820 (m), 2500 (w), 2150 (w), 1500 (s), 1420 (s), 1300 (s), 1050 (br), 980 (w), 890 (w), 850 (m), 765 (w), 720 (w).

$(Ar^{Me6})_2Ge(H)OMe$ (2). MeOH (15.9 μL, 0.3924 mmol) was dissolved in Et_2O (20 mL) and this solution was added dropwise to a slurry of $Ge(Ar^{Me6})_2$ (0.2745 g 0.3924 mmol) in Et_2O (35 mL) at −78 °C. The resulting mixture was stirred and allowed to warm slowly to room temperature overnight, giving a pale purple solution. After 48 hours of stirring, a pale yellow solution was obtained. Reduction of the solvent to *ca.* 4 mL gave colorless X-ray quality crystals that contained **2** (82 %) co-crystallized with **1** (18 %). The formation of **1** presumably occurs due to presence of adventitious water. Adjusted mass yield: 53 %, 0.161 g). Mp: 189−194 °C. ^1H NMR (500 MHz, C_6D_6, 25 °C, ppm): 1.85 (s, 12H, *o*-Me), 1.86 (s, 12H, *o*-Me), 2.24 (s, 12H, *p*-Me), 2.74 (s, 3H, OMe), 5.83 (s, 1H, Ge*H*), 6.69 (d, J_{HH} = 7.5 Hz, 4H, C_6H_3) 6.81 (s, 8H, C_6H_2), 7.00 (t, J_{HH} = 7.5 Hz,

2H, C_6H_3). $^{13}C\{^1H\}$ NMR (151 MHz, C_6D_6, 25 °C, ppm): 21.20 (*p*-CH_3), 22.11 (*o*-CH_3), 22.17 (*o*-CH_3), 128.58, 128.70, 129.67, 130.37, 136.28, 136.64, 137.16, 139.03, 141.41, 148.99. IR (cm^{-1}): 2920 (s), 2830 (s), 1450 (m), 1370 (w), 1255 (w), 1050 (br), 800 (m).

{Ar^{Me6}Sn(*μ*-OH)}$_2$ (3). H_2O (3.13 μL, 0.174 mmol) was dissolved in Et_2O (15 mL) and this solution was added dropwise to a slurry of Sn(Ar^{Me6})$_2$ (0.1300 g, 0.174 mmol) in Et_2O (40 mL) at −78 °C. The resulting mixture was stirred and allowed to warm slowly to room temperature overnight, which resulted in a slightly cloudy pale yellow solution. The solvent volume was reduced to *ca.* 5 mL after which the solution was decanted. The resulting solid was dried under reduced pressure giving a yellow powder. X-ray quality single crystals of both **3** and Ar^{Me6}H were grown from a saturated Et_2O solution. Total mass yield: 90% (0.1175 g). Upon heating, crystals of **3** become visibly orange at *ca.* 160 °C but no melting is observed < 250 °C. ^1H NMR (500 MHz, C_6D_6, 25 °C, ppm): 0.00 (s, 2H, O*H*), 2.14 (s, 24H, *o*-Me), 2.29 (s, 12H, *p*-Me) 6.83 (s, 8H, C_6H_2), 6.96 (d, J_{HH} = 7.5 Hz, 4H, C_6H_3), 7.23 (t, J_{HH} = 7.5 Hz, 2H, C_6H_3). $^{13}C\{^1H\}$ (151 MHz, C_6D_6, 25 °C, ppm): 21.46 (*p*-Me), 21.62 (*o*-Me), 128.79, 136.38, 136.50, 139.81, 146.92. IR (cm^{-1}): 2910 (s), 2855 (s), 1600 (w), 1450 (m), 1370 (m), 1255 (m), 1190 (m), 1015 (m), 840 (m), 795 (s), 730 (m), 395 (m). λ_{max} (nm, ε): 362 (700).

{Ar^{Me6}Sn(*μ*-OMe)}$_2$ (4). MeOH (13.2 μL, 0.327 mmol) was dissolved in Et_2O (15 mL) and this solution was added dropwise to a slurry of Sn(Ar^{Me6})$_2$ (0.2438 g, 0.327 mmol) in Et_2O (40 mL) at *ca.* −78 °C. The resulting mixture was stirred and allowed to warm to room temperature overnight, which afforded a yellow solution. Filtration via cannula and evaporation of the solvent gave a mixture of **4** and Ar^{Me6}H as a yellow powder. Single crystals of **4** suitable for X-ray diffraction were grown from a saturated Et_2O solution. Total mass yield: 93.3% (0.2373 g). Mp: 127−129 °C. ^1H NMR (500 MHz, C_6D_6, 25° C, ppm): 2.16 (s, 24H, *o*-Me), 2.22 (s, 12H, *p*-Me), 2.37 (s, 6H, OMe), 6.79 (s, 8H, C_6H_2), 6.94 (d, J_{HH} = 7.5 Hz, 4H, C_6H_3), 7.19 (t, 2H, C_6H_3). $^{13}C\{^1H\}$ (151 MHz, C_6D_6, 25 °C, ppm): 21.20 (*p*-Me), 22.03 (*o*-Me), 51.81 (OMe), 128.95, 129.32, 136.16, 136.18, 140.79, 147.91, 178.24. IR (cm^{-1}): 2890 (s), 2700 (w), 1590 (w), 1440 (s), 1360 (s), 1240 (m), 1100 (br), 830 (w), 780 (m), 700 (m), 360 (w). λ_{max} (nm, ε): 337 (1600).

Computational Details. All calculations were performed with Gaussian09.[32] The structures of the studied systems were optimized using the PBE1PBE hybrid exchange-correlation functional[33] in conjunction with the def-TZVP basis sets.[34] For tin, a def2-TZVP basis with an effective core potential (ECP) was used to treat scalar relativistic effects.[35] Dispersion interactions were modelled by applying Grimme's empirical dispersion correction with Becke-Johnson damping (D3BJ).[36] The choice of a particular functional-basis set combination was motivated by our recent theoretical-experimental studies of the chemistry of metallylenes as well as computational efficiency.[2a, 8, 14] The correction for dispersion effects was considered crucial in order to obtain accurate energetics for systems employing bulky terphenyl substituents.

Calculations were performed only for the reactions of heavier tetrylenes with water. Model compounds based on the Ar^{Me4} ligand (Ar^{Me4} = C_6H_3-2,6-{C_6H_3-2,6-$(CH_3)_2$}$_2$) were used to reduce the computational cost. The nature of stationary points found (minimum or transition state) was assessed with calculation of full Hessian matrices using analytic or numerical gradients.

ASSOCIATED CONTENT

Supporting Information

Crystallographic information files for **1–4**, synthetic details of deuterium analogues **1′** and **3′**, and additional spectroscopic (NMR, IR, and UV/Vis) and computational data.

AUTHOR INFORMATION

Corresponding Authors

* E-mail: pppower@ucdavis.edu
* E-mail: heikki.m.tuononen@jyu.fi

Notes

The authors declare no competing financial interest.

ACKNOWLEDGMENT

We are grateful to the U.S. Department of Energy (DE-FG02-07ER46475; P.P.P.) and the Academy of Finland (136929, 253907, and 272900; H.M.T.) for funding. P.V. thanks the Fulbright Center for a personal scholarship.

REFERENCES

(1) Mizuhata, Y.; Sasamori, T.; Tokitoh, N. *Chem. Rev.* **2009**, *109*, 3479–3511.

(2) (a) Protchenko, A. V.; Birjkumar, K. H.; Dange, D.; Schwarz, A. D.; Vidovic, D.; Jones, C.; Kaltsoyannis, N.; Mountford, P.; Aldridge, S. *J. Am. Chem. Soc.* **2012**, *134*, 6500–6503. (b) Rekken, B. D.; Brown, T. M.; Fettinger, J. C.; Tuononen, H. M.; Power, P. P. *J. Am. Chem. Soc.* **2012**, *134*, 6504–6507.

(3) (a) Al-Rafia, S. M. I.; Malcolm, A. C.; Liew, S: K.; Ferguson, M. J.; Rivard, E. *J. Am. Chem. Soc.* **2011**, *133*, 777–779. (b) Thimer, K. C.; Al-Rafia, S. M. I.; Ferguson, M. J.; McDonald, R.; Rivard, E. *Chem. Commun.* **2009**, 7119–7121.

(4) (a) Li, J.; Schenk, C.; Goedecke, C.; Frenking, G.; Jones, C. *J. Am. Chem. Soc.* **2011**, *133*, 18622–18625. (b) Pu, L.; Twamley, B.; Power, P. P. *J. Am. Chem. Soc.* **2000**, *122*, 3524-3525. (c) Peng, Y.; Fischer, R. C.; Merrill, W. A.; Fischer, J.; Pu, L.; Ellis, B. D.; Fettinger, J. C.; Herber, R. H.; Power, P. P. *Chem. Sci.* **2010**, *1*, 461–468.

(5) Wang, X.; Zhu, Z.; Peng, Y.; Lei, H.; Fettinger, J. C.; Power, P. P. *J. Am. Chem. Soc.* **2009**, *131*, 6912–6913.

(6) (a) Peng, Y.; Guo, J.-D.; Ellis, B. D.; Zhu, Z.; Fettinger, J. C.; Nagase, S.; Power, P. P. *J. Am. Chem. Soc.* **2009**, *131*, 16272–16282. (b) Peng, Y.; Ellis, B. D.; Wang, X.; Power, P. P. *J. Am. Chem. Soc.* **2008**, *130*, 12268–12269.

(7) (a) Wang, W.; Inoue, S.; Yao, S.; Driess, M. *Organometallics* **2011**, *30*, 6490–6494. (b) Jana, A.; Roesky, H. W.; Schulzke, C.; Samuel, P. P. *J. Am. Chem. Soc.* **2009**, *131*, 4600–4601. (c) Jana, A.; Objartel, I.; Roesky, H. W.; Stalke, D. *Inorg. Chem.* **2009**, *48*, 798–810.

(8) Lips, F.; Fettinger, J. C.; Mansikkamäki, A.; Tuononen, H. M.; Power, P. P. *J. Am. Chem. Soc.* **2013**, *136*, 634–637.

(9) Xiong, Y.; Yao, S.; Brym, M.; Driess, M. *Angew. Chem. Int. Ed.* **2007**, *46*, 4511–4513.

(10) Inomata, K.; Watanabe, T.; Miyazaki, Y.; Tobita, H. *J. Am. Chem. Soc.* **2015**, *137*, 11935–11937.

(11) Protchenko, A. V.; Blake, M. P.; Schwarz, A. D.; Jones, C.; Mountford, P.; Aldridge, S. *Organometallics* **2015**, *34*, 2126–2129.

(12) Power, P. P. *Acc. Chem. Res.* **2011**, *44*, 627–637.

(13) Simons, R. S.; Pu, L.; Olmstead, M. M.; Power, P. P. *Organometallics*, **1997**, *16*, 1920–1925.

(14) (a) Brown, Z. D.; Vasko, P.; Erickson, J. D.; Fettinger, J. C.; Tuononen, H. M.; Power, P. P. *J. Am. Chem. Soc.* **2013**, *135*, 6257–6261. (b) Brown, Z. D.; Vasko, P.; Fettinger, J. C.; Tuononen, H. M.; Power, P. P. *J. Am. Chem. Soc.* **2012**, *134*, 4045–4048.
(15) Brown, Z. D.; Guo, J. D.; Nagase, S.; Power, P. P. *Organometallics* **2012**, *31*, 3768–3772.
(16) Brown, Z. D.; Erickson, J. D.; Fettinger, J. C.; Power, P. P. *Organometallics* **2013**, *32*, 617–622.
(17) Erickson, J. D.; Fettinger, J. C.; Power, P. P. *Inorg Chem.* **2015**, 54, 1940–1948.
(18) For some recent examples, see: (a) Billone, P. S.; Beleznay, K.; Harrington, C. R.; Huck, L. A.; Leigh, W. J. *J. Am. Chem. Soc.* **2011**, *133*, 10523–10534. (b) Becerra, R.; Cannady, J. P.; Walsh, R. *J. Phys. Chem. A* **2011**, *115*, 4231–4230. (c) Leigh, W. J.; Kostina, S. S.; Bhattacharya, A.; Moiseev, A. G. *Organometallics* **2010**, *29*, 662–670. (d) Leigh, W. J.; Lollmahomed, F.; Harrington, C. R.; McDonald, J. M. *Organometallics* **2006**, *25*, 5424–5434. (e) Alexander, U. N.; King, K. D.; Lawrance, W. D. *Phys. Chem. Chem. Phys.* **2003**, *5*, 1557–1561. (f) Becerra, R.; Cannady, J. P.; Walsh, R. *J. Phys. Chem. A* **2003**, *107*, 11049–11056. (g) Alexander, U. N.; King, K. D.; Lawrance, W. D. *J. Phys. Chem. A* **2002**, *106*, 973–981. (h) Heaven, M. W.; Metha, G. F.; Buntine, M. A. *Aust. J. Chem.* **2001**, *54*, 185–192. (i) Heaven, M. W.; Metha, G. F.; Buntine, M. A. *J. Phys. Chem. A* **2001**, *105*, 1185–1196. (j) Duffy, I. R.; Leigh, W. J. *Organometallics* **2015**, *34*, 5029–5044.
(19) Lappert, M. F.; Miles, S. J.; Atwood, J. L.; Zaworotko, M. J.; Carty, A. J. *J. Organomet. Chem.* **1981**, *212*, C4–C6.
(20) Schager, F.; Goddard, R.; Seevogel, K.; Pörschke, K.-R. *Organometallics* **1998**, *17*, 1546–1551.
(21) Sweeder, R. D.; Miller, K. A.; Edwards, F. A.; Wang, J.; Banaszak Holl, M. M.; Kampf, J. W. *Organometallics* **2003**, *22*, 5054–5062.
(22) Hadlington, T. J.; Hermann, M.; Frenking, G.; Jones, C. *Chem. Sci.* **2015**, 6, 7249-7257.
(23) Pu, L.; Hardman, N. J.; Power, P. P. *Organometallics* **2001**, *20*, 5105–5109.
(24) Li, L.; Fukawa, T.; Matsuo, T.; Hashizume, D.; Fueno, H.; Tanaka, K.; Tamao, K. *Nature Chem.* **2012**, *4*, 361–365.
(25) Niemeyer, M.; Power, P. P. *Organometallics* **1997**, *16*, 3258-3250.
(26) (a) Summerscales, O. T.; Olmstead, M. M.; Power, P. P. *Organometallics* **2011**, *30*, 3468–3471. (b) Spikes, G. H.; Peng, Y.; Fettinger, J. C.; Steiner, J.; Power, P. P. *Chem. Commun.* **2005**, 6041–6043.
(27) Waterman, R. *Organometallics* **2013**, *32*, 7249–7263.
(28) Kostina, S. S.; Singh, T.; Leigh, W. J. *J. Phys. Org. Chem.* **2011**, *24*, 937–946.
(29) Steele, K. P.; Weber, W. P. *J. Am. Chem. Soc.* **1980**, *102*, 6095–6097.
(30) Huck, L. A.; Leigh, W. J. *Can. J. Chem.* **2011**, *89*, 241–255.
(31) Pangborn, A. B.; Giardello, M. A.; Grubbs, R. H.; Rosen, R. K.; Timmers, F. J. *Organometallics* **1996**, *15*, 1518–1520.
(32) Frisch, M. J.; Trucks, G. W.; Schlegel, H. B.; Scuseria, G. E.; Robb, M. A.; Cheeseman, J. R.; Scalmani, G.; Barone, V.; Mennucci, B.; Petersson, G. A.; Nakatsuji, H.; Caricato, M.; Li, X.; Hratchian, H. P.; Izmaylov, A. F.; Bloino, J.; Zheng, G.; Sonnenberg, J. L.; Hada, M.; Ehara, M.; Toyota, K.; Fukuda, R.; Hasegawa, J.; Ishida, M.; Nakajima, T.; Honda, Y.; Kitao, O.; Nakai, H.; Vreven, T.; Montgomery Jr., J. A.; Peralta, J. E.; Ogliaro, F.; Bearpark, M. J.; Heyd, J.; Brothers, E. N.; Kudin, K. N.; Staroverov, V. N.; Kobayashi, R.; Normand, J.; Raghavachari, K.; Rendell, A. P.; Burant, J. C.; Iyengar, S. S.; Tomasi, J.; Cossi, M.; Rega, N.; Millam, N. J.; Klene, M.; Knox, J. E.; Cross, J. B.; Bakken, V.; Adamo, C.; Jaramillo, J.; Gomperts, R.; Stratmann, R. E.; Yazyev, O.; Austin, A. J.; Cammi, R.; Pomelli, C.; Ochterski, J. W.; Martin, R. L.; Morokuma, K.; Zakrzewski, V. G.; Voth, G. A.; Salvador, P.; Dannenberg, J. J.; Dapprich, S.; Daniels, A. D.; Farkas, Ö.; Foresman, J. B.; Ortiz, J. V.; Cioslowski, J.; Fox, D. J. Gaussian 09, Revision D.01, Gaussian, Inc.: Wallingford, CT, USA, 2009.
(33) (a) Adamo, C.; Barone, V. *J. Chem. Phys.* **1999**, *110*, 6158–6170. (b) Perdew, J. P.; Burke, K.; Ernzerhof, M. *Phys. Rev. Lett.* **1997**, *78*, 1396. (c) Perdew, J. P.; Burke, K.; Ernzerhof, M. *Phys. Rev. Lett.* **1996**, *77*, 3865–3868. (d) Perdew, J. P.; Ernzerhof, M.; Burke, K. *J. Chem. Phys.* **1996**, *105*, 9982–9985.
(34) Schaefer, A.; Huber, C.; Ahlrichs, R. *J. Chem. Phys.* **1994**, *100*, 5829–5835.
(35) (a) Metz, B.; Stoll, H.; Dolg, M. *J. Chem. Phys.* **2000**, *113*, 2563–2569. (b) Weigend, F.; Ahlrichs, R. *Phys. Chem. Chem. Phys.* **2005**, *7*, 3297–3305.
(36) (a) Grimme, S.; Ehrlich, S.; Goerigk, L. *J. Comput. Chem.* **2011**, *32* (7), 1456–1465. (b) Grimme, S.; Antony, J.; Ehrlich, S.; Krieg, H. *J. Chem. Phys.* **2010**, *132*, 154104–154119.